KSCE Journal of Civil Engineering (2019) 23(8):3493-3508

DOI 10.1007/s12205-019-1588-7

Structural Engineering

pISSN 1226-7988, eISSN 1976-3808
www.springer.com/12205

A Design Formula for Lateral Load Resistance of Concrete Filled Double-Steel-Plate Walls with Small Height-to-Length Ratio

Mojtaba Labibzadeh* and Reza Hamidi**

Received August 9, 2018/Revised March 28 2019/Accepted June 2, 2019/Published Online July 8, 2019

Abstract

This study was designed to find an analytical formula for predicting the ultimate shear strength of a novel kind of complex steel-concrete shear walls known as double steel plate complex shear wall (DSCSW). The performance of these compound walls is now under research and no adequate design provisions are available. Three types of analytical formulae consisting of full shear yield, local and global shear elastic buckling were proposed and their precisions were investigated. To this end, a comprehensive 3D nonlinear finite element (FE) parametric analysis was performed. To carry out such parametric study, 120 FE models of DSCSWs were simulated and analyzed using ABAQUS package. All models were constructed according to an FE model of a test sample of DSCSW which had been constructed and tested in 2013 by Rafiei. The validity of that FE model was verified by comparing the simulation results with the experimental results. The variables considered in the parametric study were the profiled steel plate thickness, the compressive strength of infill concrete, the yield strength of the profiled steel plate and finally the number of the intermediate fasteners. At the end of this study, it was revealed that the full shear yield formula can provide a good estimation of the shear capacity of this type of shear walls when at least one row of the intermediate fasteners in the mid-height of the wall used for connecting the steel plates to the concrete panel.

Keywords: *double steel plate complex shear wall, analytical relations, shear strength, numerical simulation, full shear yielding, local and global elastic shear buckling, concrete failure*

1. Introduction

Functioning of steel plate shear walls (SPWs) has been examined in a lot of scientific papers until now. The latest most cited ones are Vian and Bruneau, 2004; Deylami and Rowghani-Kashani, 2011; Kurata *et al.,* 2012; Borello and Fahnestock, 2013; Yadollahi *et al.,* 2015; Clayton *et al.,* 2016; Pavir and Shekastehband, 2017; Hoseinzadeh Asl and Sfarkhani, 2017; Zhang *et al.,* 2018; Afshari and Gholhaki, 2018; Farzampour *et al.,* 2018; Tong and Guo, 2018; Jin and Bai, 2019; Hajimirsadeghi *et al.,* 2019; Wang *et al.,* 2019.

By reviewing the above-mentioned studies, it can be found that the main shortcoming of the SPWs is the premature out-of-plane elastic buckling of such plates which restricts their performance in energy dissipation. One solution for improving the buckling resistance of the SPWs is to increase the plate thickness. This solution results in an increase of the weight of the structure and therefore is uneconomical. Another solution for preventing of elastic buckling of SPWs is to use horizontal, vertical or diagonal stiffeners. This method, on the other hand, demands high executive cost due to welding operations needed for joining the stiffeners to the wall. In recent years, two new approaches have been developed to overcome the above-mentioned deficiencies. The first solution is to use of profiled steel plates instead of flat steel plates, and the second is to fasten two profiled steel plates to a concrete core by fasteners. This second obtained wall is called double steel plate complex shear wall or in abbreviated form as DSCSW.

The first paper introduced and discussed the concept of the DSCSWs published in 1987. Wright *et al.* (1987) suggested the utilization of the compound steel-concrete slabs as the floor members in the construction of the steel frame structures. Wright and Evans (1995) investigated the possibility of the use of the DSCSWs to absorb the energy received by a steel structure during the earthquake excitations. Hossain and Wright (1998) performed some experimental tests on DSCSW. After an interruption, Hossain and Wright (2004), resumed their studies on this type of shear walls. Hossain *et al.* (2016) intended to examine the performance of DSCSW inclusively. Hossain and his team work built some test samples of DSCSWs in the laboratory and investigated the performance of them under the action of various types of loading. They concluded at the end of their research that the general failure reason of DSCSWs is the yielding of the steel sheets accompanied with the post-yield buckling. They also

*Associate Professor, Dept. of Civil Engineering, Faculty of Engineering, Shahid Chamran University of Ahvaz, Ahvaz, Iran (Corresponding Author, E-mail: labibzadeh_m@scu.ac.ir)
**M.Sc. Student, Dept. of Civil Engineering, Faculty of Engineering, Shahid Chamran University of Ahvaz, Ahvaz, Iran (E-mail: reza.hamidi100@gmail.com)

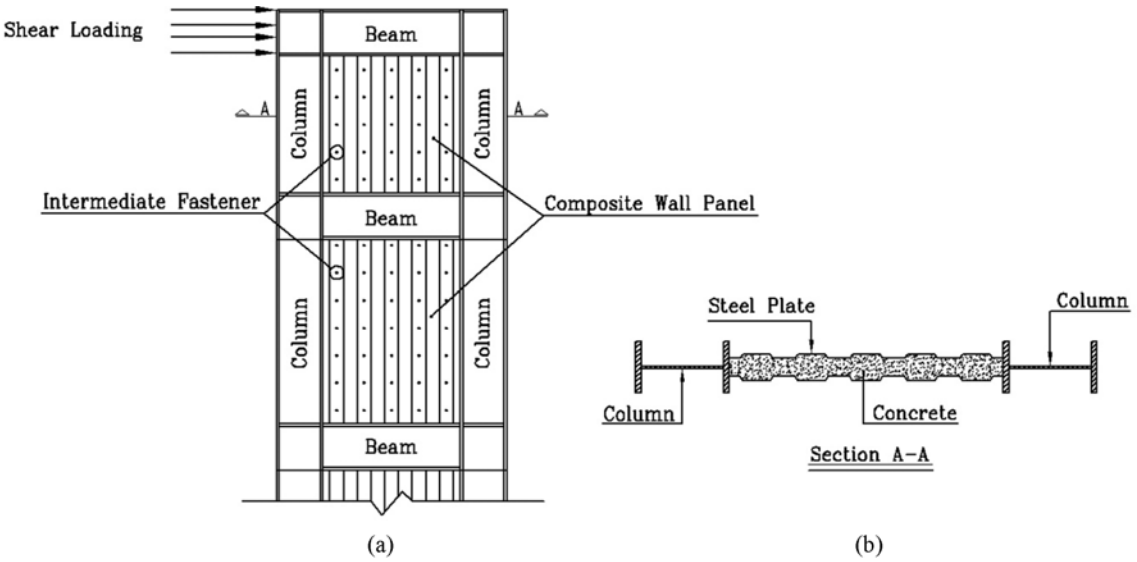

Fig. 1. DSCSW Lateral-Resisting System: (a) Simplified Picture of a Frame Strengthened Laterally with DSCSWs, (b) Cross Area Items of DSCSW

reported that the load bearing capacity of DSCSWs is not reduced significantly under cyclic loading and displacement ductility of DSCSWs is lower than the traditional steel shear walls. In recent years, a number of researchers have conducted experimental and numerical studies on the behavior of DSCSWs. Among them, Nie *et al.,* 2014; Hilo *et al.,* 2015; Yan *et al.,* 2018; Tong *et al.,* 2018; Qin *et al.,* 2019; Rafiei *et al.,* 2017; Hossain *et al.,* 2016; Yang *et al.,* 2016; Labibzadeh and Hamidi, 2019 are the latest ones.

In DSCSWs, the two external profiled steel sheets are playing the role of formwork system on construction stage and after hardening of the internal concrete core, the whole system of the steel sheets and infill concrete acts as a vertical or lateral load resisting structural member (see Fig. 1).

The experimental studies of Hossain and his co-workers are very valuable and established a platform for performing numerical parametric researches on DSCSWs in order to make the experimental findings more practical and applicable. It is worth to mention that design provisions for this type of composite steel shear walls have not been developed yet. This was the main reason that motivated the authors of this paper to do such a parametric study. The objective of this study is to introduce proper analytical relations and then evaluate the precision of them in predicting the shear capacity of DSCSWs.

2. Proposed Analytical Relations for Shear Capacity of DSCSWs

Mechanical behavior of the DSCSWs like any other structural member depends on two important factors; material behavior and loading condition. The structure of the DSCSWs is composed of two profiled steel plates and a concrete panel. The loading condition which has been studied in this paper is the pure in-plane shear load. Under this condition, three failure modes for steel plates can be occurred: full shear yielding, local elastic shear buckling or global elastic shear buckling. Presence of the concrete panel prevents the steel plates from the inward buckling, so the plates can only buckle in the outward direction. This phenomenon is considered in the following suggested buckling relationships based on the available conducted researches. At the following, the theoretical relations which are needed for computing the shear capacity of the DSCSWs will be presented.

2.1 Shear Capacity of a Profiled Steel Plate

Although Mahendran (1994) and Mezzomo (2014) carried out valuable research on the buckling and the load carrying capacity of the corrugated thin steel plates, they considered only the loads which applied perpendicular to the surface or plane of the plate. In other words, they focused on the plates which are going to be used as a roof structural system. Zimmermann (2006) performed an investigation on the local and global buckling of the curved thin steel plates under in-plane deformations, but in this study, the load and deformation were considered in the vertical direction which makes the plate to be subjected to compressions such as a column or gravity wall. However, in the current study, the behavior of the DSCSWs under the shear loads is intended to be examined. Therefore, at the following, only those studies are reviewed which investigated the shear buckling and shear capacity of the profiled steel plates.

2.1.1 Full Shear Yielding

In DSCSWs, when the intermediate fasteners provide sufficient lateral supports to prevent early elastic buckling of the profiled steel plate, the shear capacity of the steel plate can be calculated using von-Mises failure criterion. With respect to the loading condition and geometry of the DSCSWs, in this study, the pure

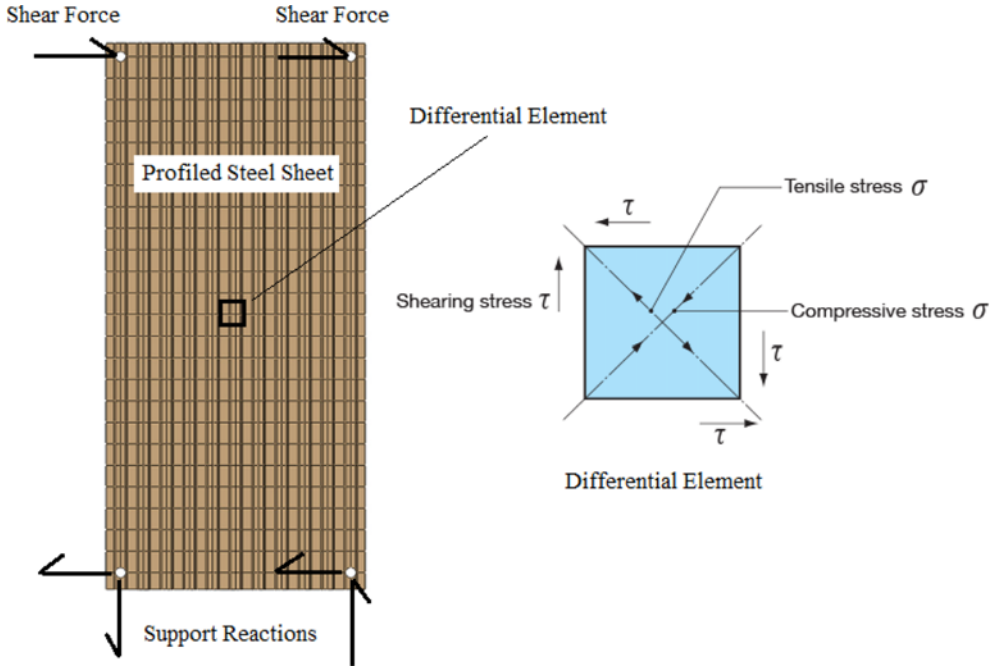

Fig. 2. Profiled Steel Sheet under In-plane Shear Load

shear of the plane stress version of the von-Mises criterion of the profiled steel sheets should be used as follows (Rafiei, 2011):

$$\sigma_{von-Mises} = \left\{ \frac{(\sigma_x - \sigma_y)^2 + \sigma_x^2 + \sigma_y^2 + 6\tau^2}{2} \right\}^{\frac{1}{2}} = f_y \quad (1)$$

In the above equation, σ_x and σ_y are the plane normal stresses and τ is the shear stress, which are acting on a two dimensional differential element located on the steel sheet (Fig. 2). f_y is the yield stress of the steel. In pure shear, σ_x and σ_y become zero and only τ remains. Hence, the Eq. (1) for pure shear state of the stress reduces to:

$$(3\tau^2)^{\frac{1}{2}} = f_y \rightarrow \tau_y = \frac{f_y}{\sqrt{3}} = 0.577 f_y \quad (2)$$

According to shear stress obtained in Eq. (2), the shear capacity of one profiled steel sheet can be calculated as follows:

$$V_s = \tau_y \cdot A_s = 0.577 f_y \cdot A_s = 0.577 f_y \cdot l_w \cdot t_s \quad (3)$$

In which, V_s denotes the shear capacity of steel sheet, A_s is the cross-sectional area of the steel sheet, l_w denotes the projected length of the sheet and t_s refers to the thickness of the sheet (See Fig. 3).

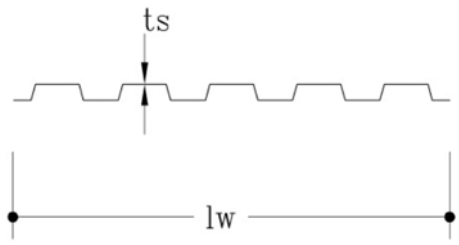

Fig. 3. Schematic Cross-sectional Area of a Profiled Steel Plate

2.1.2 Local Elastic Shear Buckling

The criterion stated by the Eq. (2) is valid only when the elastic buckling of the steel sheet is not occurring before yielding. If under the effect of compressive stress developed in the diagonal direction of a differential element (see Fig. 2), resulted from shear stress in horizontal direction, the profiled steel plate buckles locally in the elastic region, the Eq. (2) cannot be used. Rafiei (2011) based on the classical theory of buckling of thin plates of Timoshenko, 1961, assumed the critical local buckling shear stress value ($\tau_{cr,l}$) for the case of the simple support condition as below:

$$\tau_{cr,l} = k_v \frac{\pi^2 E_s}{12(1-v_s^2)} \left(\frac{t_s}{b}\right)^2 \leq \frac{f_y}{\sqrt{3}} = 0.577 f_y \quad (4)$$

$$k_v = 4\left(\frac{b}{a}\right)^2 + 5.34 \quad (5)$$

In the above equations, k_v is the local shear buckling coefficient, which its value is dependent on the boundary conditions and rectangular panel's aspect ratio ($\frac{b}{a}$), E_s is the Young modulus of the steel sheet, υ_s is the Poisson's ratio of the sheet, t_s denotes the thickness of the sheet and finally a and b are the larger and smaller dimensions of a rectangular panel of the sheet respectively. Fig. 4 shows a rectangular panel (a flat sub-plate between vertical edges) in three different arrangements of the intermediate stiffeners.

Based on the Eq. (4), if a rectangular panel buckles before the yielding is reached, the shear capacity of the plate is computed according to the below equation:

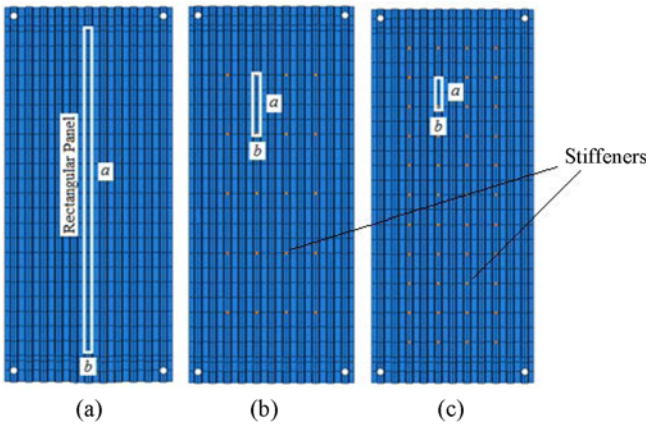

Fig. 4. Rectangular Panels: (a) No Intermediate Fastener, (b) 20 Intermediate Fasteners, (c) 44 Intermediate Fasteners

$$V_s = \tau_{cr,l} \cdot A_s = k_v \frac{\pi^2 E_s}{12(1-\upsilon_s^2)} \left(\frac{t_s}{b}\right)^2 l_w \cdot t_s \tag{6}$$

According to the findings of Eldib (2009), Local buckling occurs when a rectangular panel has a large width-to-thickness ratio ($\frac{b}{t_s}$).Global buckling mode can also be occurred depending on the geometric characteristics of the sheet (see Fig. 5). Unfortunately, until today, an analytical formula which can predict which one of the above-mentioned buckling modes will happen in a profiled steel plate before performing FE analysis has not been developed by scientists.

Elbid (2009), Yadollahi (2015) and Bahrebar (2016) proposed the same relation as Rafiei (2011) suggested for computing the local buckling coefficient when the supports of rectangular panel are simple. Furthermore, these researchers proposed a relation for determining the parameter k_v if the supports are assumed clamped:

$$k_v = 5.6\left(\frac{b}{a}\right)^2 + 8.98 \tag{7}$$

In addition, Yadollahi (2015), proposed the below relation when the long edges of the rectangular panel have simple and short edges have clamped support condition:

$$k_v = 5.34 + 2.31\left(\frac{b}{a}\right) - 3.44\left(\frac{b}{a}\right)^2 + 8.39\left(\frac{b}{a}\right)^2 \tag{8}$$

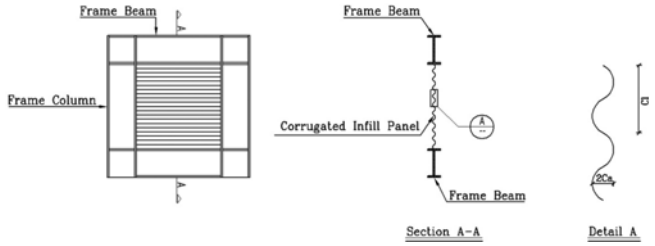

Fig. 6. Sinusoidal Corrugated Steel Plate

Dou (2016) recently presented a formula similar to relation (4) for computing of elastic local shear buckling of sinusoidal corrugated steel plates as below:

$$\tau_{cr,l} = k_l \frac{\pi^2 E_s}{12(1-\upsilon_s^2)} \left(\frac{t}{s_c/2}\right)^2 \tag{9}$$

In which S_c can be obtained using the following equation:

$$S_c = C_1 \sqrt{1 + 16.3\left(\frac{c_a}{c_1}\right)^{1.92}} \tag{10}$$

Parameters C_a and C_1 are corrugation depth and corrugation wavelength respectively, which are shown in Fig. 6 and t denotes the thickness of the plate.

k_l represents the local buckling coefficient computed as follows (Duo, 2016):

$$k_l = c + d\left(\frac{c_a}{c_1}\right) \tag{11}$$

$$c = 5.16 + 0.539\left(\frac{C_a}{t}\right) - 0.00614\left(\frac{C_a}{t}\right)^2 - \frac{11.2}{\left(\frac{L}{C_1}\right)} + \frac{32.6}{\left(\frac{L}{C_1}\right)^2} + 0.762\frac{\left(\frac{C_a}{t}\right)}{\left(\frac{L}{C_1}\right)} \tag{12}$$

$$d = 0.816 - 5.27\left(\frac{c_a}{t}\right)^{0.5} \tag{13}$$

In the current study, relations (9) to (13) will be used for calculation of the local elastic shear buckling of the profiled steel plate in DSCSWs with this notification that C_a is replaced by h and C_1 is substituted with (b + e + 2d) (see Fig. 7). Based on the

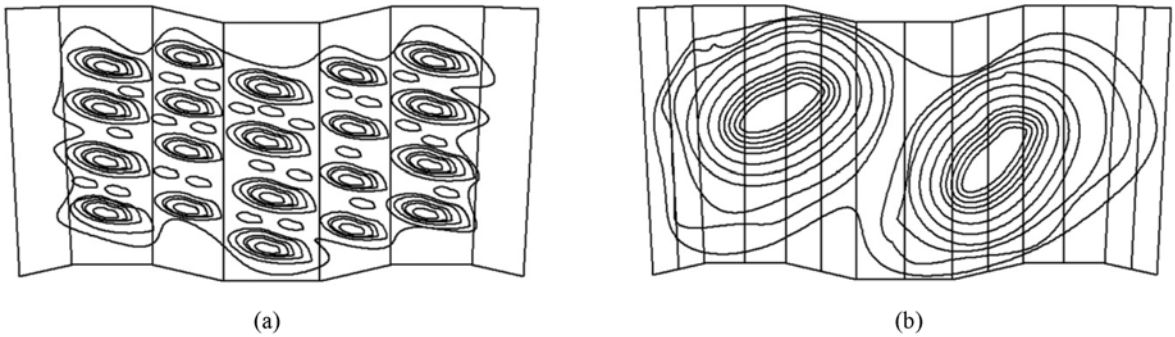

Fig. 5. Different Buckling Modes of the Profiled Steel Sheet: (a) Local Buckling, (b) Globel Buckling

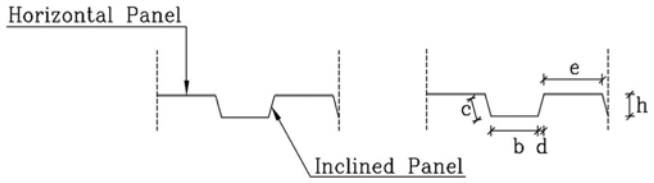

Fig. 7. Geometric Characteristics of Trapezoidal Corrugated Plate

relations (4) to (13), the shear capacity of a profiled steel plate which buckles locally can be calculated as follows:

$$V_s = \tau_{cr,l} \cdot A_s = \tau_{cr,l} \cdot l_w \cdot t_s \tag{14}$$

2.1.3 Global Elastic shear Buckling

If under the effect of the shear load, a corrugated trapezoidal steel sheet buckles globally, Yadollahi (2015) and Tong and Guo (2015) based on a theoretical solution presented earlier by Easley (1975) suggested that the global shear buckling stress ($\tau_{cr,g}$) can be calculated as follows:

$$\tau_{cr,g} = k_g \frac{D_x^{1/4} D_y^{3/4}}{L^2 t_s} \tag{15}$$

In which D_x and D_y are the bending rigidities per unit length of the steel corrugated trapezoidal sheet with bending moment directions parallel and perpendicular to the corrugation line respectively. These parameters have been calculated as follows (Yadollahi, 2015):

$$D_x = \frac{E t_s^3}{12(1-\vartheta^2)} \frac{b+d}{b+c} \tag{16}$$

$$D_y = \frac{E t_s h^2}{12} \frac{3b+c}{b+d} \tag{17}$$

In relations (16) and (17), b is the width of a horizontal panel, c is the smaller dimension of inclined panel, d is the projected length of c and h denotes the depth of the corrugated plate (See Fig. 7).

L is the effective buckling length of the steel sheet which is dependent of its boundary conditions and aspect ratio. t_s denotes the thickness of the sheet and finally k_g represents the global shear buckling coefficient. Yadollahi *et al.* (2015) suggested the value of 68.4 for k_g and Tong and Guo (2015) proposed a relation for computing k_g as follow:

$$k_g = (7+20\theta)\beta^2 + 8\beta + 61.2 + 29.5\theta \tag{18}$$

$$\theta = \frac{D_{xy}}{\sqrt[2]{D_x D_y}}, \beta = \frac{L}{H}\sqrt[4]{\frac{D_x}{D_y}}, D_{xy} = \frac{s}{c_1} \frac{E t_s^3}{6(1+\vartheta)} \tag{19}$$

S in the above relation denotes the developed length of one repeating corrugation; $S = 2(b+c)$, and C_l referrers to the projected length of one repeating corrugation. Based on the Eqs. (15) to (19), the shear capacity of a profiled steel plate of DSCSW which buckles globally is obtained as below:

$$V_s = \tau_{cr,g} \cdot A_s = \tau_{cr,g} \cdot l_w \cdot t_s \tag{20}$$

2.2 Shear Capacity of the Concrete Panel

Shear strength of the concrete infill panel was computed in the present study using the below equations (Rafiei, 2011):

$$V_c = \beta \sqrt{f_c} t_c d_v \tag{21}$$

$$\beta = \frac{0.4}{1+1,500\varepsilon_y} \tag{22}$$

$$\varepsilon_y = \frac{\frac{M}{d_v} + 0.5N + V}{2A_C E_S} \tag{23}$$

In the above relations, f_c is the compressive strength of 28-days cured standard cylindrical concrete sample, t_c denotes the average thickness of the equivalent rectangular of the profiled concrete panel, d_v is the effective shear depth of profiled concrete panel, β is defined as shear retention factor which is calculated by relation (22), ε_y presents the longitudinal strain at mid-depth of the concrete panel can be derived by Eq. (23), M denotes the bending moment about the strong axis of the composite wall, N is axial load perpendicular to the cross-section of the wall, V is shear load, E_s shows the Young's modulus of steel column and A_c represents the cross-sectional area of the steel column.

2.3 Total Shear Capacity of the DSCSW

According to the relations presented for shear capacities of the profiled steel plate and concrete panels in the previous sub-sections, the total shear capacity of a DSCSW (V_w) can be obtained as below:

$$V_w = V_s + V_c \tag{24}$$

The above relation is valid when the composite action between the concrete panel and the steel plates is fully developed. That means the in-plane displacements of the concrete panel and the steel plates are compatible. If any shear sliding is occurred between these two parts, the validity of the Eq. (24) becomes violated. So, a sufficient numbers of the intermediate fasteners is required to connect the steel plates to the concrete panel in order to prevent such a shear sliding.

3. FE Modeling as a Tool for Verification of the Proposed Analytical Relations

In the current study, 120 number of Double Skin Concrete composite Steel plate shear Walls- DSCSWs- have been modeled in order to perform the necessary parametric study. Results of the parametric study were used for verification of the proposed analytical relations presented in section 2. The commercial finite element software, ABAQUS, was employed for simulating the above-mentioned 120 walls. For the parametric study, DSCSWs with four distinct thicknesses of steel face plate (t_s = 0.6, 0.8, 1.0 and 1.20 mm), five different arrangements of the intermediate fasteners (0, 4, 12, 20, and 44 fasteners), three different concrete compressive strengths (f_c = 20, 35 and 60 MPa) and two different steel yield strengths (f_y = 354 and 552 MPa) were considered in this study.

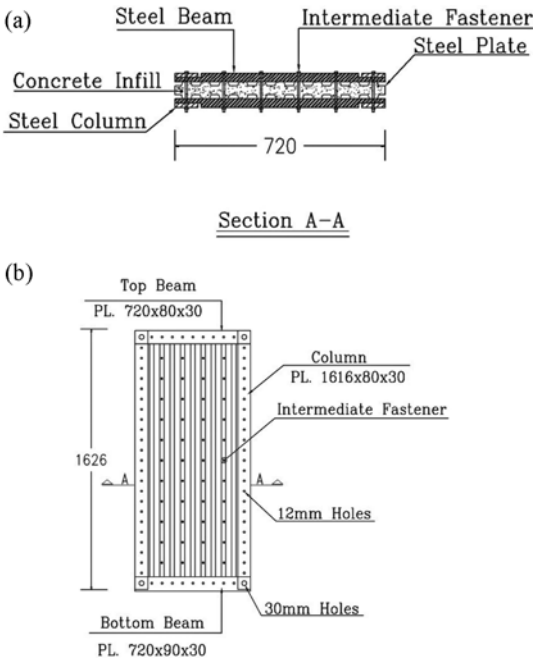

Fig. 8. The Geometric Characteristics of the Model Simulated in ABAQUS (mm): (a) Cross Section Details, (b) Profile of the Wall

3.1 Geometry of DSCSWs for Parametric Study

In the current study, for performing a comprehensive parametric study on the behavior of DSCSWs, the laboratory sample used by Rafiei *et al.* (2013) was chosen and simulated using ABAQUS package. The geometrics of this sample were horizontally 720 mm and vertically 1,626 mm. The items of the wall and circumferential frame are illustrated in Fig. 8.

3.2 Constitute Relations for Concrete

Concrete damage plasticity model, CDP, was implemented in the current study to simulate the performance of the concrete material. The input variables employed in CDP model were considered according to Labibzadeh, 2015 to labibzadeh, 2018.

3.3 Steel Material Model

For steel material modeling, the characteristics used by Rafiei (2013) were implemented in this study. According to this reference, for mild strength steel, the initial and ultimate yield stresses were considered as 354 and 484 MPa respectively. The corresponding plastic strains were defined as 0.0 and 0.212781 mm/mm respectively. The modulus of elasticity was set as 206.980 MPa. For high strength steel, the initial and ultimate stresses and their corresponding plastic strains were set as 552 MPa, 624 MPa, 0.0 mm/mm and 0.089516 mm/mm respectively. The Young modulus of high strength steel was defined as 202.940 MPa.

3.4 Element Types and Inter-connection Algorithms

The S4R shell elements were assigned for simulation of the steel sheets in DSCSWs. Brick elements of kind C3D8R were employed for concrete panel and the load frame. In order to model the shear connectors which bond the steel plates to the concrete infill, the tie constraint was implemented. By this approach, the out-of-plane displacements of the profiled steel sheets in the location of the fasteners are prohibited. After performing several sensitivity analyses on the size of the elements, the optimum length of the C3D8R elements was obtained as 50 millimeters.

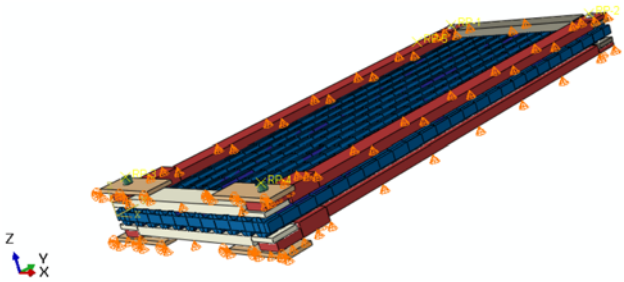

Fig. 9. Restrictions on Deformations Applied in the Wall Model

3.5 Boundary Conditions

The out-of-plane deformations of the frame was turned aside to guarantee the in-plane behavior of the wall. All the three displacement degrees of freedom (DOF) of the bottom side of the steel supports were restrained. At the location of the circumferential bolts which connect the load frame, steel sheets and concrete panel to each other, the out-of-plane deformations were removed (see Fig. 9).

3.6 Solving Strategy

The dynamic explicit step of the ABAQUS package was considered for performing the analyses due to the existence of the large amount of the interactions between different parts of the model.

3.7 Applied Forces

To provide a capability to pursue the post-peak performance of the DSCSW, a deformation measurable protocol was employed to apply the shear forces to the wall. The loading was applied by specifying a reference point which was placed in the center line of the four 30 mm bolts (rigid pins) and assigning a prescribed horizontal displacement (80 mm) to that reference point. The reference point was coupled kinematically with the cross-sections of the rigid pins (see Fig. 10). By this way, the displacements of the

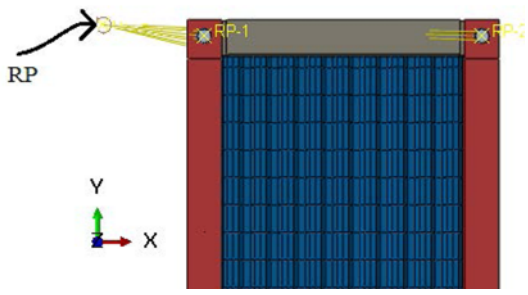

Fig. 10. Reference Point for Inserting the Predefined Deformations to the Wall

4 mentioned pins are the same and quantitatively are equal to the displacements of the reference point. This 80 mm displacement is applied gradually and steadily (without inertia effects) in the horizontal direction (along the x-axis) and in the plane of the composite wall (parallel to x-y coordinate plane).

4. Justifying the Numerical Model against Experiment

The force-deformation relationship obtained from the numerical analysis is compared to that of the experimental one in Fig. 11. It is worth mentioning that both of the displacement and the load are considered in the horizontal direction and they are both located in the plane of the composite shear wall. In other words, the displacement and load are parallel and measured in the plane of the wall. The load is obtained by the summation of the horizontal in-plane reactions of the nodes located in the bottom of the restrained planes shown by red color in Fig. 9. According to Fig. 11, a reasonable coincidence between the numerical and experimental results can be found. The percentage of difference for the shear capacity is near to 3.2% and for deformation is approximately 0.5%.

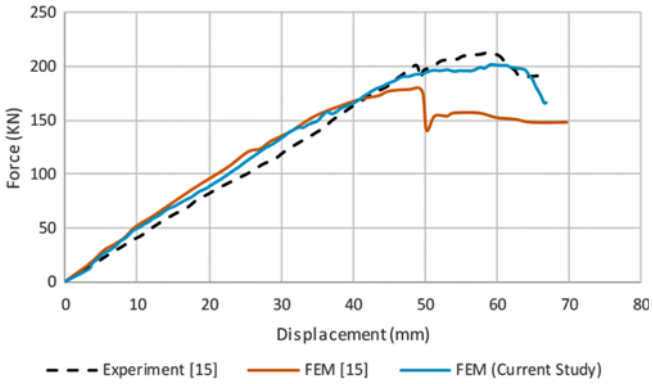

Fig. 11. Force-Deformation Relationships of the Current Study and Those of Rafiei *et al.,* 2013

Furthermore, as it is observed from the above picture, the force-deformation trend of the composite wall is nearly linear from the beginning of the loading up to the failure stage. This demonstrates that the behavior of this composite wall with these dimensions is pure shear and the mode of the failure is shear failure. No flexural behavior is developed within the wall. If the internal bending moment is developed within the wall, then the load-displacement curve would be obtained curvilinear. It is worth to mention that the height-to-length ratio of the composite shear wall in this study is about 1536/720 or 2. If this ratio reaches to values considerably greater than 2, then the flexural action of the wall becomes noticeable and should be considered in shear capacity prediction.

According to Fig. 12, it reveals that almost all regions of the steel sheets experience the plastic deformations at the failure state (f_y = 354 MPa). This demonstrated that no elastic shear buckling (local or global) has been occurred in the profiled steel plates before the peak load is reached. If the buckling has occurred in the steel plates, some regions of the plates should be under the yield shear stress limit. This conclusion can be justified when observing the Fig. 13. In this figure, the out-of-plane displacement of profiled steel plates obtained from the FE model in different stages of the load-displacement curve of Fig. 11 is depicted. In Fig. 13, the force-deformation relationship of the FE model which has been shown earlier in Fig. 11 with the blue curve, is illustrated again. Points (b) to (f) on this curve indicate different stages of the loading. As it can be seen from Fig. 13, from stage (b) to (d) there is a stable and small out-of-plane deformation in the plate. During these stages, as the lateral displacement of the wall increases, the load carried by the wall is also increased. Stage (d) denotes the peak of the load moment in the load-displacement diagram. As it can be seen from Fig. 12, in this moment, all

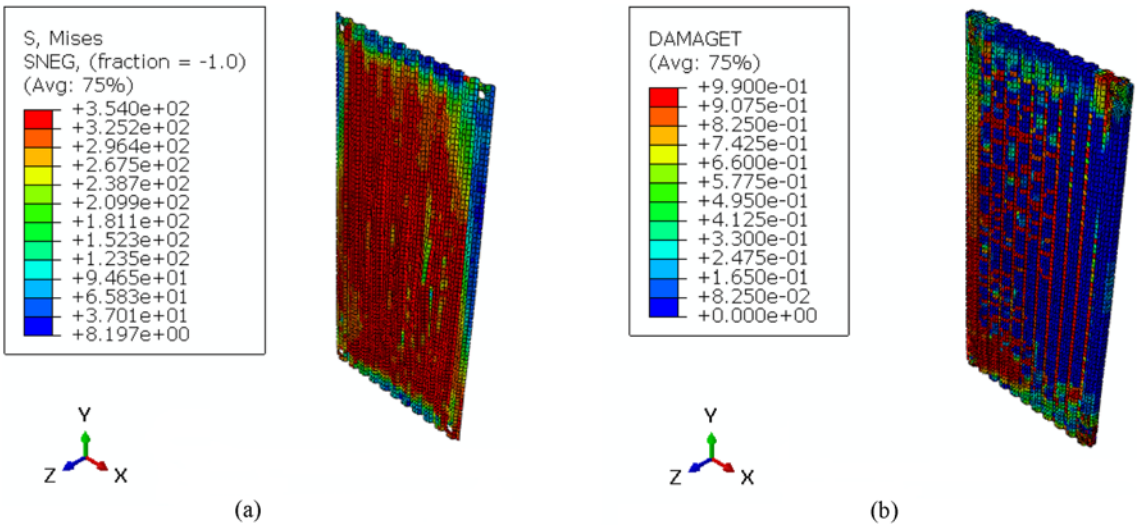

Fig. 12. Configurations of Developed Stresses and Cracks in the Wall: (a) Von-Mises Stresses in Steel Plates, (b) Tensile Damages in Concrete Panel

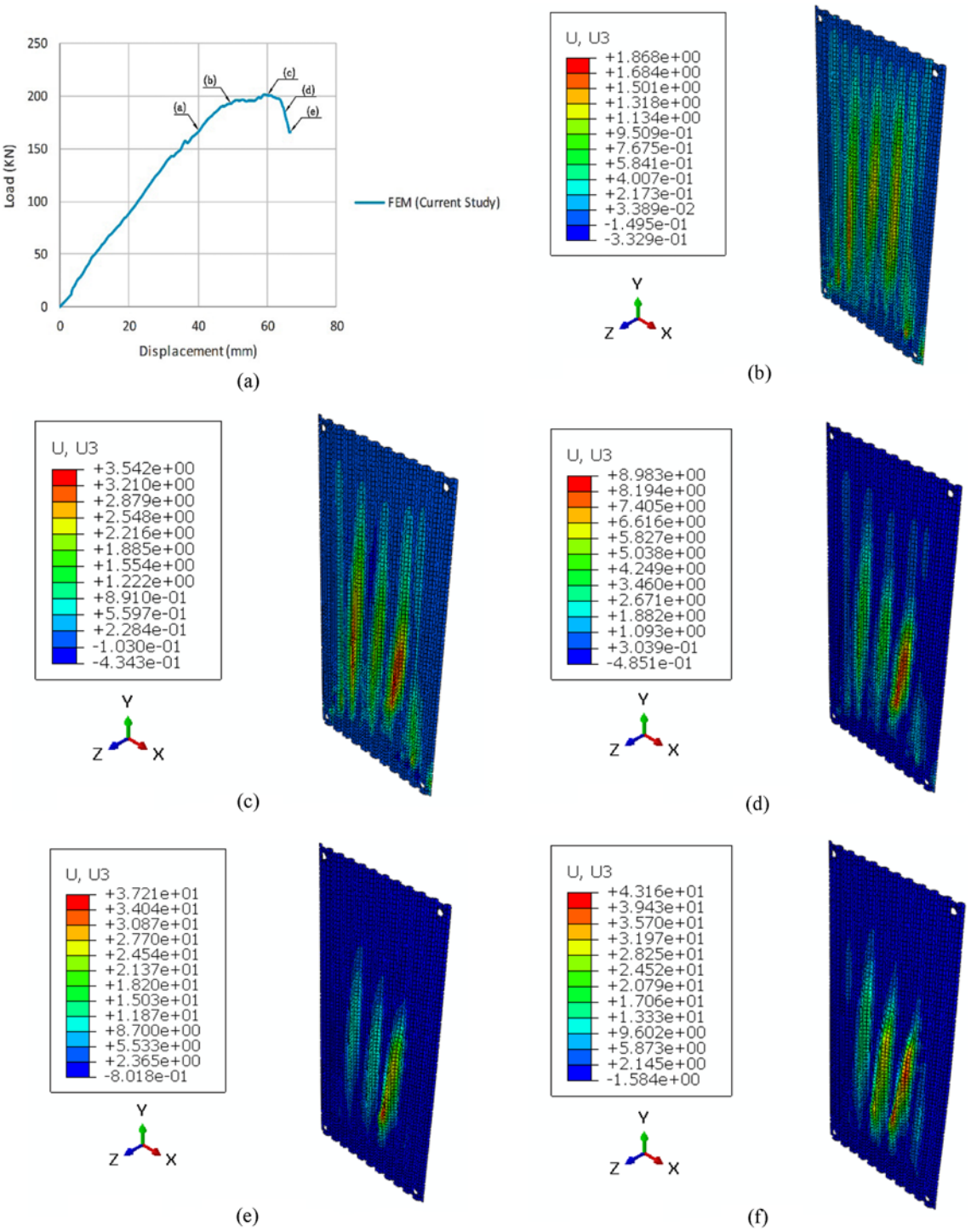

Fig. 13. Out-of-plane Displacement of DSCSW in Different Stages of Shear Loading: (a) Force-Deformation Relationship of the FE Model, (b) and (c) before the Peak Load, (d) At the Peak Load, (e) and (f) after the Peak Load

points of the plate reach approximately to the shear yield stress. From stage (d) to the next stage, i.e., stage (e), the out-of-plane displacement of the plate shows a sudden rise. During this step, the plate buckles plastically. This reveals that before the peak of the load is reached, no elastic buckling can be occurred in the plate. This simulation result is in complete agreement with the experimental observation reported by Rafiei *et al.* (2013).

Buckling modes of the profiled steel plates is illustrated in Fig. 14. These buckling shapes are obtained by performing a modal analysis in ABAQUS software. In this figure, the first six modes of the composite wall is illustrated. As it can be observed from this figure, none of these buckling modes is occurred in Fig. 13 before the peak load is reached. Hence, there is no buckling before the ultimate load-carrying capacity of the DSCSWs in this study.

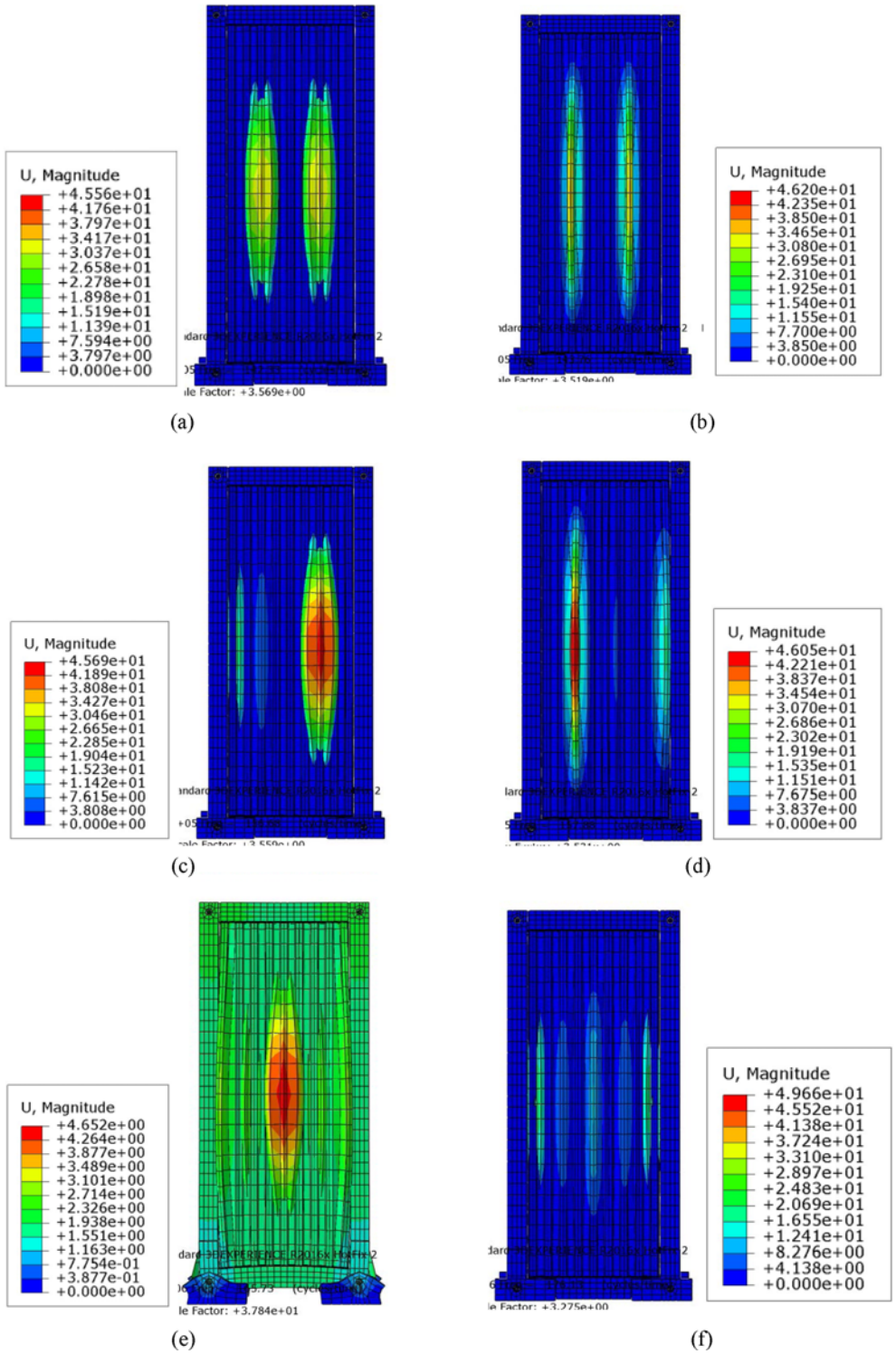

Fig. 14. Buckling Modes of the DSCSW Obtained from a Modal Analysis of ABAQUS: (a) to (f) = The First to Sixth Buckling Modes, Respectively.

5. Results of Parametric Study

As it was mentioned in the introduction part, a comprehensive parametric study has been performed in the current study in order to investigate the precisions of the proposed analytical relations provided in section 2 of this article. 120 FE models were developed and analyzed using ABAQUS/CAE/Explicit v6.14. These models were labeled in order to sake of the brevity in the presentation of the results in the following tables and figures. For example 'MS-CCS 20-TS 0.61-IF 0'denotes a

Table 1. Parametric Study Results of DSCSWs for f_y = 354 Mpa, f_c = 20 MPa

f_y = 354 MPa – f_c = 20 MPa									
<1> Name of DSCSWs	V_c (kN) Analytical	V_s (kN)– Analytical					V_w (kN)	V_w (kN)	<10> Error (%)
	<2> Eq. (21)	<3> Eq. (4)	<4> Eq. (9)	<5> Eq. (3)	<6> Design stress	<7> V_s (kN) - Eqs. (3) or (14)	<8> Analytical-Eq. (24) = <2> + <7>	<9> FEM	
MS-CCS 20-TS 0.61-IF 0	31.50	509.38	394.28	204.38	204.38	179.53	211.03	216.17	2.38
MS-CCS 20-TS 0.61-IF 4	31.20	510.44	394.28	204.38	204.38	179.53	210.73	221.69	4.94
MS-CCS 20-TS 0.61-IF 12	31.20	510.44	394.28	204.38	204.38	179.53	210.73	221.42	4.83
MS-CCS 20-TS 0.61-IF 20	31.00	513.62	394.28	204.38	204.38	179.53	210.53	225.70	6.72
MS-CCS 20-TS 0.61-IF 44	30.90	526.35	394.28	204.38	204.38	179.53	210.43	226.17	6.96
MS-CCS 20-TS 0.8-IF 0	29.20	876.11	595.05	204.38	204.38	235.45	264.65	260.82	1.47
MS-CCS 20-TS 0.8-IF 4	28.40	877.94	595.05	204.38	204.38	235.45	263.85	277.59	4.95
MS-CCS 20-TS 0.8-IF 12	28.50	877.94	595.05	204.38	204.38	235.45	263.95	276.11	4.41
MS-CCS 20-TS 0.8-IF 20	28.50	883.41	595.05	204.38	204.38	235.45	263.95	276.13	4.41
MS-CCS 20-TS 0.8-IF 44	28.50	905.31	595.05	204.38	204.38	235.45	263.95	276.47	4.53
MS-CCS 20-TS 1.0-IF 0	27.20	1368.92	843.11	204.38	204.38	294.31	321.51	307.77	4.46
MS-CCS 20-TS 1.0-IF 4	26.40	1371.77	843.11	204.38	204.38	294.31	320.71	328.02	2.23
MS-CCS 20-TS 1.0-IF 12	26.30	1371.77	843.11	204.38	204.38	294.31	320.61	330.03	2.85
MS-CCS 20-TS 1.0-IF 20	26.30	1380.33	843.11	204.38	204.38	294.31	320.61	330.45	2.98
MS-CCS 20-TS 1.0-IF 44	26.30	1414.55	843.11	204.38	204.38	294.31	320.61	330.33	2.94
MS-CCS 20-TS 1.2-IF 0	25.30	1971.25	1129.48	204.38	204.38	353.17	378.47	357.62	5.83
MS-CCS 20-TS 1.2-IF 4	24.50	1975.35	1129.48	204.38	204.38	353.17	377.67	380.16	0.65
MS-CCS 20-TS 1.2-IF 12	24.40	1975.35	1129.48	204.38	204.38	353.17	377.57	382.96	1.41
MS-CCS 20-TS 1.2-IF 20	24.50	1987.67	1129.48	204.38	204.38	353.17	377.67	380.97	0.86
MS-CCS 20-TS 1.2-IF 44	24.40	2036.95	1129.48	204.38	204.38	353.17	377.57	384.61	1.83

DSCSW composed of two mild strength corrugated steel plates with the yield strength of f_y = 354 MPa, a concrete panel with a compressive strength of f_c = 20 MPa, the plate thickness of 0.61 mm and no intermediate fasteners, and MS-CCS 20-TS 0.8-IF 20 stands for the same composite shear wall with the plate thickness of 0.8 mm and 20 intermediate fasteners. Tables 1 to 6 summarized the results of the parametric study investigating the precision of the analytical formulae. In these tables, column <1>introduces the names of the shear walls, column<2> presents the analytical shear capacities of concrete panels -V_c (kN)- using Eq. (21), column <3> denotes the local shear buckling stress of the steel plates using Eq. (4) from, column <4> includes local

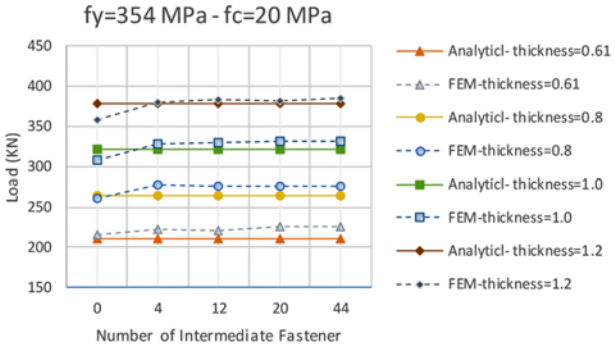

Fig. 15. Comparisons of Analytical and FEM Shear Load Capacities of DSCSWs for Different Numbers of Fasteners and Plate Thicknesses - f_y = 354 MPa, f_c = 20 MPa

Table 2. Parametric Study Results of DSCSWs for f_y = 354 MPa, f_c = 35 MPa

f_y = 354 MPa – f_c = 35 MPa									
<1> Name of DSCSWs	V_c (kN) Analytical	V_s (kN) – Analytical					V_w (kN)	V_w (kN)	<10> Error (%)
	<2> Eq. (21)	<3> Eq. (4)	<4> Eq. (9)	<5> Eq. (3)	<6> Design stress	<7> V_s (kN)-Eqs. (3) or (14)	<8> Analytical-Eq. (24) = <2> + <7>	<9> FEM	
MS-CCS 35.7-TS 0.61-IF 0	41.10	509.38	394.28	204.38	204.38	179.53	220.63	229.39	3.82
MS-CCS 35.7-TS 0.61-IF 4	40.50	510.44	394.28	204.38	204.38	179.53	220.03	238.47	7.73
MS-CCS 35.7-TS 0.61-IF 12	40.70	510.44	394.28	204.38	204.38	179.53	220.23	236.19	6.76
MS-CCS 35.7-TS 0.61-IF 20	40.40	513.62	394.28	204.38	204.38	179.53	219.93	240.57	8.58
MS-CCS 35.7-TS 0.61-IF 44	40.40	526.35	394.28	204.38	204.38	179.53	219.93	240.07	8.39
MS-CCS 35.7-TS 0.8-IF 0	38.20	876.11	595.05	204.38	204.38	235.45	273.65	275.39	0.63
MS-CCS 35.7-TS 0.8-IF 4	37.50	877.94	595.05	204.38	204.38	235.45	272.95	286.41	4.70

Table 2. (continued)

f_y = 354 MPa – f_c = 35 MPa									
<1> Name of DSCSWs	V_c (kN) Analytical	V_s (kN) – Analytical					V_w (kN)	V_w (kN)	<10> Error (%)
	<2> Eq. (21)	<3> Eq. (4)	<4> Eq. (9)	<5> Eq. (3)	<6> Design stress	<7> V_s (kN)-Eqs. (3) or (14)	<8> Analytical-Eq. (24) = <2> + <7>	<9> FEM	
MS-CCS 35.7-TS 0.8-IF 12	37.60	877.94	595.05	204.38	204.38	235.45	273.05	284.77	4.11
MS-CCS 35.7-TS 0.8-IF 20	37.30	883.41	595.05	204.38	204.38	235.45	272.75	289.55	5.80
MS-CCS 35.7-TS 0.8-IF 44	37.40	905.31	595.05	204.38	204.38	235.45	272.85	288.65	5.48
MS-CCS 35.7-TS 1.0-IF 0	35.40	1368.92	843.11	204.38	204.38	294.31	329.71	324.25	1.68
MS-CCS 35.7-TS 1.0-IF 4	34.40	1371.77	843.11	204.38	204.38	294.31	328.71	344.24	4.51
MS-CCS 35.7-TS 1.0-IF 12	34.50	1371.77	843.11	204.38	204.38	294.31	328.81	342.99	4.13
MS-CCS 35.7-TS 1.0-IF 20	34.50	1380.33	843.11	204.38	204.38	294.31	328.81	343.66	4.32
MS-CCS 35.7-TS 1.0-IF 44	34.40	1414.55	843.11	204.38	204.38	294.31	328.71	345.30	4.80
MS-CCS 35.7-TS 1.2-IF 0	32.80	1971.25	1129.48	204.38	204.38	353.17	385.97	378.23	2.05
MS-CCS 35.7-TS 1.2-IF 4	32.20	1975.35	1129.48	204.38	204.38	353.17	385.37	393.72	2.12
MS-CCS 35.7-TS 1.2-IF 12	32.10	1975.35	1129.48	204.38	204.38	353.17	385.27	394.67	2.38
MS-CCS 35.7-TS 1.2-IF 20	32.20	1987.67	1129.48	204.38	204.38	353.17	385.37	392.00	1.69
MS-CCS 35.7-TS 1.2-IF 44	32.10	2036.95	1129.48	204.38	204.38	353.17	385.27	395.85	2.67

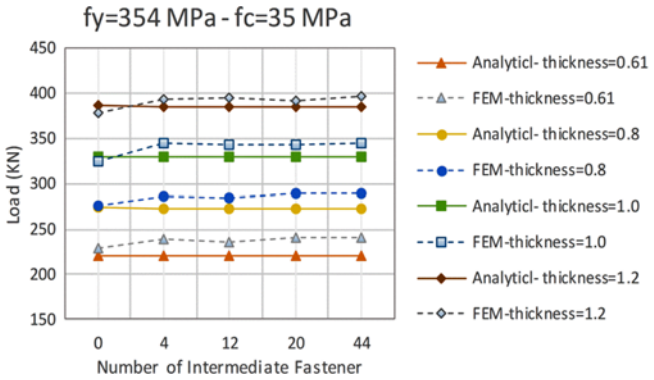

Fig. 16. Comparisons of Analytical and FEM Shear Load Capacities of DSCSWs for Different Numbers of Fasteners and Plate Thicknesses-f_y = 354 MPa, f_c = 35 MPa

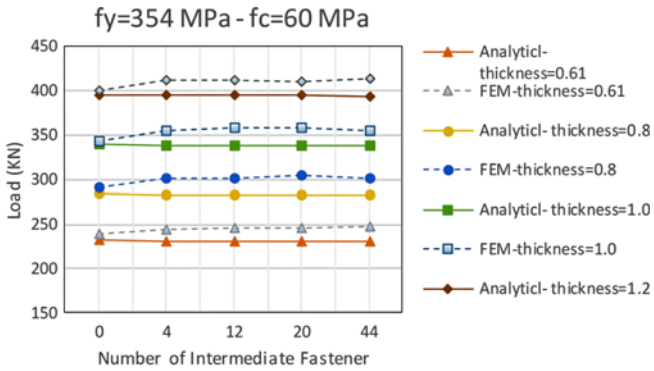

Fig. 17. Comparisons of Analytical and FEM Shear Load Capacities of DSCSWs for Different Numbers of Fasteners and Plate Thicknesses-f_y = 354 MPa, f_c = 60 MPa

Table 3. Parametric Study Results of DSCSWs for f_y = 354 MPa, f_c = 60 MPa

f_y = 354 MPa – f_c = 60 MPa									
<1> Name of DSCSWs	V_c (kN) Analytical	V_s (kN)– Analytical					V_w (kN)	V_w (kN)	<10> Error (%)
	<2> Eq. (21)	<3> Eq. (4)	<4> Eq. (9)	<5> Eq. (3)	<6> Design stress	<7> V_s (kN)-Eqs. (3) or (14)	<8> Analytical-Eq. (24) = <2> + <7>	<9> FEM	
MS-CCS 60-TS 0.61-IF 0	52.50	509.38	394.28	204.38	204.38	179.53	232.03	238.52	2.72
MS-CCS 60-TS 0.61-IF 4	52.00	510.44	394.28	204.38	204.38	179.53	231.53	244.16	5.17
MS-CCS 60-TS 0.61-IF 12	51.90	510.44	394.28	204.38	204.38	179.53	231.43	245.65	5.79
MS-CCS 60-TS 0.61-IF 20	51.90	513.62	394.28	204.38	204.38	179.53	231.43	245.95	5.90
MS-CCS 60-TS 0.61-IF 44	51.70	526.35	394.28	204.38	204.38	179.53	231.23	247.53	6.58
MS-CCS 60-TS 0.8-IF 0	48.30	876.11	595.05	204.38	204.38	235.45	283.75	291.02	2.50
MS-CCS 60-TS 0.8-IF 4	47.50	877.94	595.05	204.38	204.38	235.45	282.95	301.53	6.16
MS-CCS 60-TS 0.8-IF 12	47.60	877.94	595.05	204.38	204.38	235.45	283.05	300.22	5.72
MS-CCS 60-TS 0.8-IF 20	47.30	883.41	595.05	204.38	204.38	235.45	282.75	303.99	6.99
MS-CCS 60-TS 0.8-IF 44	47.50	905.31	595.05	204.38	204.38	235.45	282.95	301.68	6.21
MS-CCS 60-TS 1.0-IF 0	44.70	1368.92	843.11	204.38	204.38	294.31	339.01	343.04	1.17

Table 3. (continued)

f_y = 354 MPa – f_c = 60 MPa									
<1> Name of DSCSWs	V_c (kN) Analytical	V_s (kN)– Analytical					V_w (kN)	V_w (kN)	<10> Error (%)
	<2> Eq. (21)	<3> Eq. (4)	<4> Eq. (9)	<5> Eq. (3)	<6> Design stress	<7> V_s (kN)-Eqs. (3) or (14)	<8> Analytical-Eq. (24) = <2> + <7>	<9> FEM	
MS-CCS 60-TS 1.0-IF 4	43.90	1371.77	843.11	204.38	204.38	294.31	338.21	355.39	4.83
MS-CCS 60-TS 1.0-IF 12	43.80	1371.77	843.11	204.38	204.38	294.31	338.11	358.55	5.70
MS-CCS 60-TS 1.0-IF 20	43.80	1380.33	843.11	204.38	204.38	294.31	338.11	357.24	5.35
MS-CCS 60-TS 1.0-IF 44	43.90	1414.55	843.11	204.38	204.38	294.31	338.21	355.40	4.84
MS-CCS 60-TS 1.2-IF 0	41.40	1971.25	1129.48	204.38	204.38	353.17	394.57	400.27	1.42
MS-CCS 60-TS 1.2-IF 4	40.80	1975.35	1129.48	204.38	204.38	353.17	393.97	410.99	4.14
MS-CCS 60-TS 1.2-IF 12	40.80	1975.35	1129.48	204.38	204.38	353.17	393.97	411.57	4.28
MS-CCS 60-TS 1.2-IF 20	40.90	1987.67	1129.48	204.38	204.38	353.17	394.07	409.54	3.78
MS-CCS 60-TS 1.2-IF 44	40.70	2036.95	1129.48	204.38	204.38	353.17	393.87	412.39	4.49

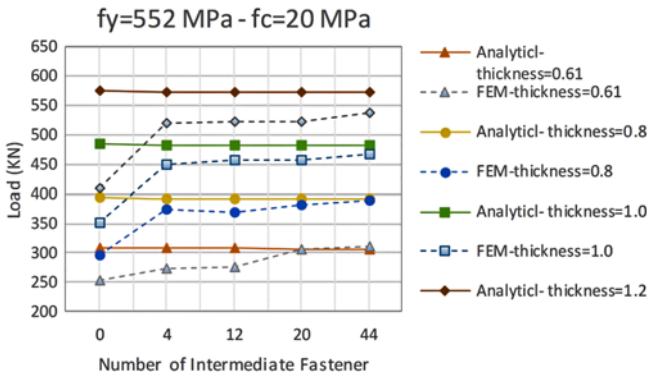

Fig. 18. Comparisons of Analytical and FEM Shear Load Capacities of DSCSWs for Different Numbers of Fasteners and Plate Thicknesses-f_y = 552 MPa, f_c = 20 MPa

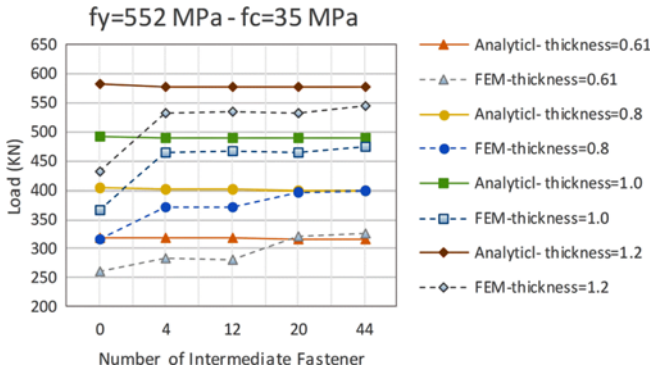

Fig. 19. Comparisons of Analytical and FEM Shear Load Capacities of DSCSWs for Different Numbers of Fasteners and Plate Thicknesses-f_y = 552 MPa, f_c = 35 MPa

Table 4. Parametric Study Results of DSCSWs for f_y = 552 MPa, f_c = 20 MPa

f_y = 552 MPa – f_c = 20 MPa									
<1> Name of DSCSWs	V_c (kN) Analytical	V_s (kN)– Analytical					V_w (kN)	V_w (kN)	<10> Error (%)
	<2> Eq. (21)	<3> Eq. (4)	<4> Eq. (9)	<5> Eq. (3)	<6> Design stress	<7> V_s (kN)-Eqs. (3) or (14)	<8> Analytical-Eq. (24) = <2>+<7>	<9> FEM	
HS-CCS 20-TS 0.61-IF 0	29.60	499.43	386.58	318.70	318.70	279.94	309.54	253.07	22.31
HS-CCS 20-TS 0.61-IF 4	28.60	500.47	386.58	318.70	318.70	279.94	308.54	273.16	12.95
HS-CCS 20-TS 0.61-IF 12	28.50	500.47	386.58	318.70	318.70	279.94	308.44	276.05	11.74
HS-CCS 20-TS 0.61-IF 20	27.26	503.59	386.58	318.70	318.70	279.94	307.20	306.55	0.21
HS-CCS 20-TS 0.61-IF 44	27.12	516.08	386.58	318.70	318.70	279.94	307.06	310.01	0.95
HS-CCS 20-TS 0.8-IF 0	27.66	859.01	583.44	318.70	318.70	367.14	394.80	296.93	32.96
HS-CCS 20-TS 0.8-IF 4	24.76	860.80	583.44	318.70	318.70	367.14	391.90	373.92	4.81
HS-CCS 20-TS 0.8-IF 12	24.91	860.80	583.44	318.70	318.70	367.14	392.05	369.63	6.06
HS-CCS 20-TS 0.8-IF 20	24.54	866.17	583.44	318.70	318.70	367.14	391.68	380.57	2.92
HS-CCS 20-TS 0.8-IF 44	24.28	887.64	583.44	318.70	318.70	367.14	391.42	388.47	0.76
HS-CCS 20-TS 1.0-IF 0	25.58	1342.20	826.65	318.70	318.70	458.92	484.50	350.50	38.23
HS-CCS 20-TS 1.0-IF 4	22.48	1345.00	826.65	318.70	318.70	458.92	481.40	448.67	7.30
HS-CCS 20-TS 1.0-IF 12	22.26	1345.00	826.65	318.70	318.70	458.92	481.19	456.56	5.39
HS-CCS 20-TS 1.0-IF 20	22.27	1353.39	826.65	318.70	318.70	458.92	481.19	456.21	5.48
HS-CCS 20-TS 1.0-IF 44	21.96	1386.94	826.65	318.70	318.70	458.92	480.89	467.71	2.82
HS-CCS 20-TS 1.2-IF 0	23.63	1932.77	1107.44	318.70	318.70	550.71	574.34	409.23	40.35

Table 4. (continued)

f_y = 552 MPa – f_c = 20 MPa									
<1> Name of DSCSWs	V_c (kN) Analytical	V_s (kN)– Analytical					V_w (kN)	V_w (kN)	<10> Error (%)
	<2> Eq. (21)	<3> Eq. (4)	<4> Eq. (9)	<5> Eq. (3)	<6> Design stress	<7> V_s (kN)-Eqs. (3) or (14)	<8> Analytical-Eq. (24) = <2>+<7>	<9> FEM	
HS-CCS 20-TS 1.2-IF 4	20.66	1936.80	1107.44	318.70	318.70	550.71	571.37	519.93	9.89
HS-CCS 20-TS 1.2-IF 12	20.63	1936.80	1107.44	318.70	318.70	550.71	571.34	521.37	9.58
HS-CCS 20-TS 1.2-IF 20	20.60	1948.88	1107.44	318.70	318.70	550.71	571.31	522.49	9.34
HS-CCS 20-TS 1.2-IF 44	20.25	1997.19	1107.44	318.70	318.70	550.71	570.96	537.89	6.15

shear buckling stress of the steel plates using Eq. (9), column <5> represents the shear yield stress of the steel plates using Eq. (3), column <6> shows the minimum values of the columns <3> to <5> as the design shear stress, column <7> outlines the shear capacities of the steel plates using Eqs. (3) or (14), column <8> yields the total analytical shear capacity of the composite wall using Eq. (24), which equals to the sum of the values of the column <2> and column <7>, column <9> presents the total FEA shear capacity of the composite wall and finally column <10> shows the percentage of the errors between the values of the column <8> and <9>. To provide more convenience for readers, Figs. 15 to 20 illustrate the main results of Tables 1 to 6 with proper curves.

After in-detail examination of the results presented in the above tables and figures, one can find that, except for 12 models, marked with the grey colored rows in Tables 4 to 6, the analytical relation (3) in section 2, suggested by Rafiei (2011), which assumes that the full shear yield stress occurred in the cross-section of the profiled steel plate, gives the closest results to the FEM results. These 12 models, are those composed of the high strength corrugated steel plate, f_y = 552 MPa and no intermediate stiffeners are used to connect the steel plate to the concrete panel (see Tables 4 to 6). Keeping in mind that in these 12 models, the predicted shear capacities by FEM are smaller than the corresponding values predicted by the analytical relation (3), the authors decided to consider the possibility of global shear buckling for the steel plates. Therefore, only for these models, the analytical relations suggested by Yadollahi *et al.* (2015), Eq. (15), and Tong and Guo (2015), Eq. (18), in section 2, were used for prediction of the shear capacity of the DSCSWs. The results are outlined in Table 7.

Table 5. Parametric Study Results of DSCSWs for f_y = 552 MPa, f_c = 35 MPa

f_y = 552 MPa – f_c = 35 MPa									
<1> Name of DSCSWs	V_c (kN) Analytical	V_s (kN)– Analytical					V_w (kN)	V_w (kN)	<10> Error (%)
	<2> Eq. (21)	<3> Eq. (4)	<4> Eq. (9)	<5> Eq. (3)	<6> Design stress	<7> V_s (kN)-Eqs. (3) or (14)	<8> Analytical-Eq. (24) = <2> + <7>	<9> FEM	
HS-CCS 35-TS 0.61-IF 0	39.16	499.43	386.58	318.70	318.70	279.94	319.10	259.86	22.80
HS-CCS 35-TS 0.61-IF 4	37.78	500.47	386.58	318.70	318.70	279.94	317.73	282.45	12.49
HS-CCS 35-TS 0.61-IF 12	37.85	500.47	386.58	318.70	318.70	279.94	317.79	281.38	12.94
HS-CCS 35-TS 0.61-IF 20	35.66	503.59	386.58	318.70	318.70	279.94	315.60	320.84	1.63
HS-CCS 35-TS 0.61-IF 44	35.35	516.08	386.58	318.70	318.70	279.94	315.30	326.69	3.49
HS-CCS 35-TS 0.8-IF 0	35.97	859.01	583.44	318.70	318.70	367.14	403.11	314.98	27.98
HS-CCS 35-TS 0.8-IF 4	33.14	860.80	583.44	318.70	318.70	367.14	400.28	372.60	7.43
HS-CCS 35-TS 0.8-IF 12	33.16	860.80	583.44	318.70	318.70	367.14	400.30	372.27	7.53
HS-CCS 35-TS 0.8-IF 20	32.15	866.17	583.44	318.70	318.70	367.14	399.29	395.22	1.03
HS-CCS 35-TS 0.8-IF 44	31.97	887.64	583.44	318.70	318.70	367.14	399.11	399.55	0.11
HS-CCS 35-TS 1.0-IF 0	33.41	1342.20	826.65	318.70	318.70	458.92	492.33	366.81	34.22
HS-CCS 35-TS 1.0-IF 4	29.44	1345.00	826.65	318.70	318.70	458.92	488.36	464.92	5.04
HS-CCS 35-TS 1.0-IF 12	29.41	1345.00	826.65	318.70	318.70	458.92	488.33	465.90	4.81
HS-CCS 35-TS 1.0-IF 20	29.46	1353.39	826.65	318.70	318.70	458.92	488.38	464.49	5.14
HS-CCS 35-TS 1.0-IF 44	29.15	1386.94	826.65	318.70	318.70	458.92	488.07	473.17	3.15
HS-CCS 35-TS 1.2-IF 0	30.72	1932.77	1107.44	318.70	318.70	550.71	581.42	430.62	35.02
HS-CCS 35-TS 1.2-IF 4	27.24	1936.80	1107.44	318.70	318.70	550.71	577.95	531.74	8.69
HS-CCS 35-TS 1.2-IF 12	27.15	1936.80	1107.44	318.70	318.70	550.71	577.86	534.60	8.09
HS-CCS 35-TS 1.2-IF 20	27.26	1948.88	1107.44	318.70	318.70	550.71	577.97	530.91	8.87
HS-CCS 35-TS 1.2-IF 44	26.88	1997.19	1107.44	318.70	318.70	550.71	577.59	543.67	6.24

Table 6. Parametric Study Results of DSCSWs for f_y = 552 MPa, f_c = MPa

f_y = 552 MPa – f_c = 60 MPa									
<1> Name of DSCSWs	V_c (kN) Analytical	V_s (kN)– Analytical					V_w (kN)	V_w (kN)	<10> Error (%)
	<2> Eq. (21)	<3> Eq. (4)	<4> Eq. (9)	<5> Eq. (3)	<6> Design stress	<7> V_s (kN)-Eqs. (3) or (14)	<8> Analytical-Eq. (24) = <2> + <7>	<9> FEM	
HS-CCS 60-TS 0.61-IF 0	49.25	499.43	386.58	318.70	318.70	279.94	329.20	278.92	18.03
HS-CCS 60-TS 0.61-IF 4	48.01	500.47	386.58	318.70	318.70	279.94	327.95	295.51	10.98
HS-CCS 60-TS 0.61-IF 12	47.60	500.47	386.58	318.70	318.70	279.94	327.54	301.15	8.77
HS-CCS 60-TS 0.61-IF 20	45.17	503.59	386.58	318.70	318.70	279.94	325.11	336.84	3.48
HS-CCS 60-TS 0.61-IF 44	44.75	516.08	386.58	318.70	318.70	279.94	324.70	343.29	5.42
HS-CCS 60-TS 0.8-IF 0	45.07	859.01	583.44	318.70	318.70	367.14	412.21	338.40	21.81
HS-CCS 60-TS 0.8-IF 4	42.30	860.80	583.44	318.70	318.70	367.14	409.44	384.13	6.59
HS-CCS 60-TS 0.8-IF 12	42.11	860.80	583.44	318.70	318.70	367.14	409.25	387.52	5.61
HS-CCS 60-TS 0.8-IF 20	41.14	866.17	583.44	318.70	318.70	367.14	408.28	405.20	0.76
HS-CCS 60-TS 0.8-IF 44	40.81	887.64	583.44	318.70	318.70	367.14	407.94	411.48	0.86
HS-CCS 60-TS 1.0-IF 0	41.49	1342.20	826.65	318.70	318.70	458.92	500.42	398.70	25.51
HS-CCS 60-TS 1.0-IF 4	37.98	1345.00	826.65	318.70	318.70	458.92	496.90	469.08	5.93
HS-CCS 60-TS 1.0-IF 12	37.88	1345.00	826.65	318.70	318.70	458.92	496.80	471.24	5.42
HS-CCS 60-TS 1.0-IF 20	37.71	1353.39	826.65	318.70	318.70	458.92	496.63	475.01	4.55
HS-CCS 60-TS 1.0-IF 44	37.40	1386.94	826.65	318.70	318.70	458.92	496.32	481.94	2.98
HS-CCS 60-TS 1.2-IF 0	38.11	1932.77	1107.44	318.70	318.70	550.71	588.82	466.15	26.31
HS-CCS 60-TS 1.2-IF 4	35.53	1936.80	1107.44	318.70	318.70	550.71	586.24	526.31	11.39
HS-CCS 60-TS 1.2-IF 12	35.40	1936.80	1107.44	318.70	318.70	550.71	586.10	529.62	10.66
HS-CCS 60-TS 1.2-IF 20	35.18	1948.88	1107.44	318.70	318.70	550.71	585.89	535.06	9.50
HS-CCS 60-TS 1.2-IF 44	34.47	1997.19	1107.44	318.70	318.70	550.71	585.17	553.69	5.69

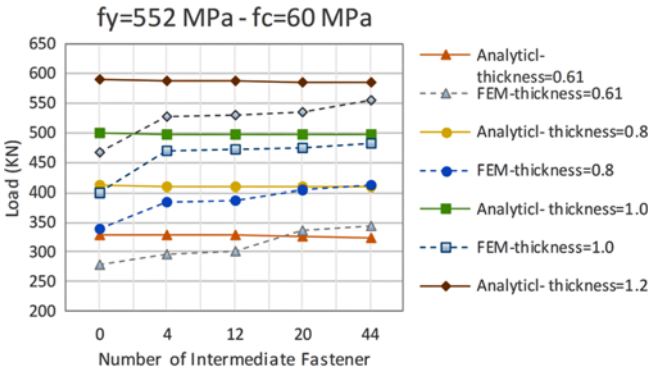

Fig. 20. Comparisons of Analytical and FEM Shear Load Capacities of DSCSWs for Different Numbers of Fasteners and Plate Thicknesses-f_y = 552 MPa, f_c = 60 MPa

It is revealed from the Table 7 that the obtained errors are much higher than the corresponding errors in Tables 4 to 6. This demonstrates that the assumption of the global buckling of the steel plates is not a precise postulation and/or the formula of the global buckling in this kind of the shear walls does not yield satisfactory results. Hence, it can be deduced that when there are no fasteners and the steel plates have high yield strength; the available analytical relations cannot be used for prediction of the shear capacity of DSCSWs. This is due to the fact that when the steel corrugated plate is not connected sufficiently to the concrete panel, if the plate has high yield strength, the stress distribution in the cross-sectional area of the steel plate is not uniform and the stresses do not reach to the shear yield stress Thus, the analytical full shear yield equation, Eq. (3), or local shear buckling formulae, Eqs. (4) and (9), overestimate the shear capacity of the wall, whereas the analytical global shear buckling formula, Eq. (15), underestimates the shear capacity. It is worth mentioning that, when there is a minimum connectivity between the steel plate and concrete panel, i.e., 4 intermediate fasteners are used in the middle height of the wall, which provide the minimum composite action of the wall, the developed stresses in the cross-section of the steel plate reach to the yield shear stress (full efficiency of the steel plate) and von-Mises criterion, Eq. (3) from Rafiei (2011) gives desirable results (related errors are less than or equal to 12%).

6. Conclusions

According to the results and discussions provided in the preceding section, it can be concluded that the analytical relations presented in section 2 for local and global elastic shear buckling of a profiled steel plate, cannot provide accurate predictions of the shear capacity of DSCSWs. However, the analytical equation developed based on the assumption of the full shear yield stress of the profiled steel plate can predict the shear capacity of DSCSWs with admissible accuracy. This is the case when a minimum connectivity between the steel plate and concrete core is provided by the intermediate fasteners (at least one row of the fasteners should be used in the mid-height of the plate). It is

Table 7. Parametric Study Results of DSCSWs for the Case of No Intermediate Fasteners

<1> Name of DSCSWs	V_c (kN) Analytical	V_s (kN) – Analytical				V_w (kN)	V_w (kN)	<9> Error (%)
	<2> Eq. (21)	<3> Yaddolahi *et al.* 2015-Eq. (15) with k_g = 68.4	<4> Tong and Guo 2015-Eq. (18)	<5> Design stress (MPa)	<6> Vs (KN)	<7> Analytical= <2> + <6>	<8> FEM	
HS-CCS 20-TS 0.61-IF 0	29.63	36.24	21.89	21.89	19.22	48.86	253.07	80.69
HS-CCS 20-TS 0.8-IF 0	27.66	41.50	25.25	25.25	29.09	56.75	296.93	80.89
HS-CCS 20-TS 1.0-IF 0	25.58	46.40	28.46	28.46	40.99	66.56	350.50	81.01
HS-CCS 20-TS 1.2-IF 0	23.63	50.83	31.43	31.43	54.31	77.94	409.23	80.95
HS-CCS 35-TS 0.61-IF 0	39.16	36.24	21.89	21.89	19.22	58.38	259.86	77.53
HS-CCS 35-TS 0.8-IF 0	35.97	41.50	25.25	25.25	29.09	65.06	314.98	79.34
HS-CCS 35-TS 1.0-IF 0	33.41	46.40	28.46	28.46	40.99	74.39	366.81	79.72
HS-CCS 35-TS 1.2-IF 0	30.72	50.83	31.43	31.43	54.31	85.03	430.62	80.25
HS-CCS 60-TS 0.61-IF 0	49.25	36.24	21.89	21.89	19.22	68.48	278.92	75.45
HS-CCS 60-TS 0.8-IF 0	45.07	41.50	25.25	25.25	29.09	74.16	338.40	78.08
HS-CCS 60-TS 1.0-IF 0	41.49	46.40	28.46	28.46	40.99	82.48	398.70	79.31
HS-CCS 60-TS 1.2-IF 0	38.11	50.83	31.43	31.43	54.31	92.42	466.15	80.17

interesting to note that, in DSCSWs, due to the profiled shape of the plates, with a fewer numbers of fasteners in comparison to the flat steel plate composite walls, the full shear yield occurred in the cross-section of the plate. This type of the shear walls with no steel bars and with considerably small numbers of the shear connectors when compared to the other kinds of composite shear walls can undertake larger lateral forces.

Acknowledgements

Not Applicable.

References

Afshari, J. M. and Gholhaki, M. (2018). "Shear strength degradation of steel plate shear walls with optional located opening." *Archives of Civil and Mechanical Engineering*, Vol. 18, No. 4, pp. 1547-1561, DOI: 10.1016/j.acme.2018.06.012.

Bahrebar, M., Kabir, M. Z., Hajsadeghi, M., Zirakian, T., and Lim, J. B. P. (2016). "Structural performance of steel plate shear wall with trapezoidal corrugations and centrally-placed square perforations." *International Journal of Steel Structures*, Vol. 16, No. 3, pp. 845-855, DOI: 10.1007/s13296-015-0116-y.

Borello, D. J. and Fahnestock, L. A. (2013). "Seismic design and analysis of steel plate shear walls with coupling." *Journal of Structural Engineering*, Vol. 139, No. 8, pp. 1263-1273, DOI: 10.1061/(ASCE)ST.1943-541X.0000576.

Clayton, P. M., Dowden, D. M., Li, C. H., Berman, J. W., Bruneau, M., Lowes, L. N., and Tsai, K. C. (2016). "Self-centering steel plate shear walls for improving seismic resilience." *Journal of Frontiers in Structural and Civil Engineering*, Vol. 10, No. 3, pp. 283-290, DOI: 10.1007/s11709-016-0344-z.

Deylami, A. and Rowghani-Kashani, J. (2011). "Analysis and design of steel plate shear walls using orthotropic membrane model." *Journal of Procedia Engineering*, Vol. 14, pp. 3338-3345, DOI: 10.1016/j.proeng.2011.07.422.

Dou, C., Jiang, Z. Q., Pi, Y. L., and Guo, Y. L. (2016). "Elastic shear buckling of sinusoidally corrugated steel plate shear wall." *Engineering Structures*, Vol. 121, pp. 136-146, DOI: 10.1016/j.engstruct.2016.04.047.

Easley, T. (1975). "Buckling formulae for corrugated metal shear diaphragms." *Journal of the Structural Division*, Vol. 101, No. 7, pp. 1403-1417.

Eldib, M. E. A.-H. (2009). "Shear buckling strength and design of curved corrugated steel webs for bridges." *Journal of Constructional Steel Research*, Vol. 65, No. 12, pp. 2129-2139, DOI: 10.1016/j.jcsr.2009.07.002.

Farzampour, A., Mansouri, I., Lee, C. H., Sim, H. B., and Hu, J. W. (2018). "Analysis and design recommendations for corrugated steel plate shear wall with a reduced beam section." *Thin-Walled Structures,* Vol. 132, pp. 658-666, DOI: 10.1016/j.tws.2018.09.026.

Hajimirsadeghi, M., Mirtaheri, M., Zandi, A. P., and Hariri-Ardebili, M. A. (2019). "Experimental cyclic test and failure modes of a full scale enhanced modular steel plate shear wall." *Engineering Failure Analysis,* Vol. 95, pp. 283-288, DOI: 10.1016/j.engfailanal.2018.09.025.

Hilo, S. J., Wan Badaruzzaman, W. H., Osman, S. A., Al-Zand, A. W., Samir, M., and Hasan, Q. A. (2015). "A state-of-the-art review on double skinned composite wall systems." *Thin-Walled Structures*, Vol. 97, pp. 74-100, DOI: 10.1016/j.tws.2015.09.007.

Hoseinzadeh Asl, M. and Safarkhani, M. (2017). "Seismic behavior of steel plate shear wall with reduced boundary beam section." *Thin-Walled Structures*, Vol. 116, pp. 169-179, DOI: 10.1016/j.tws.2017.03.014.

Hossain, K. M. A. and Wright, H. D. (1997). "In-plane shear behavior of profiled steel sheeting." *Journal of Thin Walled Structures*, Vol. 29, Nos. 1-4, pp. 79-100, DOI: 10.1016/S0263-8231(97)00016-5.

Hossain, K. M. A. and Wright, H. D. (1998). "Performance of profiled concrete shear panels." *ASCE Journal of Structural Engineering*, Vol. 124, No. 4, pp. 368-381, DOI: 10.1061/(ASCE) 0733-9445 (1998)124:4(368).

Hossain, K. M. A. and Wright, H. D. (2004). "Behavior of composite walls under monotonic and cyclic shear loading." *Structural Engineering and Mechanics*, Vol. 17, No. 1, pp. 69-85, DOI: 10.12989/sem.2004.17.1.069.

Hossain, K. M. A. and Wright, H. D. (2004). "Design aspect of double

skin profiled composite framed shear walls in construction and service stages." *ACI Structural Journal,* Vol. 101, No. 1, pp. 94-102.

Hossain, K. M. A., Rafiei, S., Lachemi, M., and Behdinan, K. (2016). "Structural performance of profiled composite wall under in-plane cyclic loading." *Engineering Structures*, Vol. 110, pp. 88-104, DOI: 10.1016/j.engstruct.2015.11.057.

Hossain, K. M. A., Rafiei, S., Lachemi, M., Behdinan, K., and Anwar, M. S. (2016). "Finite element modeling of impact shear resistance of double skin composite wall." *Thin-Walled Structures,* Vol. 107, pp. 101-118, DOI: 10.1016/j.tws.2016.06.002.

Jin, S. and Bai, J. (2019). "Experimental investigation of buckling-restrained steel plate shear walls with inclined-slots." *Journal of Constructional Steel Research*, Vol. 155, pp. 144-156, DOI: 10.1016/j.jcsr.2018.12.021.

Kurata, M., Leon, R. T., DesRoches, R., and Nakashima, M. (2012). "Steel plate shear wall with tension-bracing for seismic rehabilitation of steel frames." *Journal of Constructional Steel Research*, Vol. 71, pp. 92-103, DOI: 10.1016/j.jcsr.2011.10.026.

Labibzadeh, M. (2015). "The numerical simulations of the strengthened RC slabs with CFRPs using standard CDP material model of Abaqus code." *European Journal of Environmental and Civil Engineering*, Vol. 19, No. 10, pp. 1268-1287, DOI: 10.1080/19648189.2015.1013637.

Labibzadeh, M. and Elahifar, T. (2015). "An enhanced finite element model for reinforced concrete two-way slabs strengthened with carbon fiber reinforced polymers." *Structural Engineering International Journal*, Vol. 25, No. 1, pp. 81-90, DOI: 10.2749/101686614X14043795570093.

Labibzadeh, M., Firouzi, A., and Ghafouri, H. R. (2018). "Structural performance evaluation of an aged structure using a modified plasticity model in inverse solution method." *Inverse Problems in Science and Engineering*, Vol. 26, No. 9, pp. 1326-1355, DOI: 10.1080/17415977.2017.1400028.

Labibzadeh, M. and Hamidi, R. (2017). "Effect of stress path, size and shape on the optimum parameters of a brittle-ductile concrete model." *Engineering Structures and Technology,* Vol. 9, No. 4, pp. 195-206, DOI: 10.3846/2029882X.2017.1414636.

Labibzadeh, M. and Hamidi, R. (2019). "A comparison between shear capacities of two composite shear walls: DSCSWs and CSPSWs." *Structural Engineering International*, Vol. 29, No. 2, pp. 276-281, DOI: 10.1080/10168664.2018.1544473.

Labibzadeh, M., Zakeri, I., and Shoeib, A. (2017). "A new method for CDP input parameter optimization of the ABAQUS software guaranteeing the uniqueness and precision." *International Journal of Structural Integrity,* Vol. 8, No. 2, pp. 264-284, DOI: 10.2749/101686614X14043795570093.

Mahendran, M. (1994). "Behaviour and design of crest-fixed profiled steel roof claddings under wind uplift." *Engineering Structures*, Vol. 16, No. 5, pp. 368-376, DOI: 10.1016/0141-0296(94)90030-2.

Mezzomo, G. P., Iturrioz, I., Grigoletti, G., and Gomes, H. M. (2014). "Influence of the fixing type in the optimization of trapezoidal roofing sheets." *Journal of Constructional Steel Research*, Vol. 96, pp. 26-39, DOI: 10.1016/j.jcsr.2014.01.006.

Nie, J. G., Ma, X. W., Tao, M. X., Fan, J. S., and Bu, F. M. (2014). "Effective stiffness of composite shear wall with double plates and filled concrete." *Journal of Constructional Steel Research*, Vol. 99, pp. 140-148, DOI: 10.1016/j.jcsr.2014.04.001.

Pavir, A. and Shekastehband, B. (2017). "Hysteretic behavior of coupled steel plate shear walls." *Journal of Constructional Steel Research*, Vol. 133, pp. 19-35, DOI: 10.1016/j.jcsr.2017.01.019.

Qin, Y., Shu, G. P., Zhou, G. G., and Han, J. H. (2019). "Compressive behavior of double skin composite wall with different plate thicknesses." *Journal of Constructional Steel Research*, Vol. 157, pp. 297-313, DOI: 10.1016/j.jcsr.2019.02.023.

Rafiei, S. (2011). *Behavior of double skin profiled composite shear wall system under in-plane monotonic, cyclic and impact loadings*, PhD Dissertation, Department of Civil Engineering, Ryerson University, Toronto, Ontario, Canada.

Rafiei, S., Hossain, K. M. A., Lachemi, M., and Behdinan, K. (2017). "Impact shear resistance of double skin profiled composite wall." *Engineering Structures*, Vol. 140, pp. 267-285, DOI: 10.1016/j.engstruct.2017.02.062.

Rafiei, S., K. M. A., Hossain, Lachemi, M., Behdinan, K., and Anwar, M. S. (2013). "Finite element modeling of double skin profiled composite shear wall system under in-plane loading." *Engineering Structures*, Vol. 56, pp. 46-57, DOI: 10.1016/j.engstruct. 2013.04.014.

Tong, J. Z. and Guo, Y. L. (2015). "Elastic buckling behavior of steel trapezoidal corrugated shear walls with vertical stiffeners." *Thin Walls Structures*, Vol. 95, pp. 31-39, DOI: 10.1016/j.tws.2015.06.005.

Tong, J. Z. and Guo, Y. L. (2018). "Shear resistance of stiffened steel corrugated shear walls". *Thin-Walled Structures,* Vol. 127, pp. 76-89, DOI: 10.1016/j.tws.2018.01.036.

Tong, J. Z., Guo, Y. L., and Zuo, J. Q. (2018). "Elastic buckling and load-resistant behaviors of double-corrugated-plate shear walls under pure in-plane shear loads." *Thin-Walled Structures,* Vol. 130, pp. 593-612, DOI: 10.1016/j.tws.2018.06.021.

Vian, D. and Bruneau, M. (2004). *Testing of special LYS steel plate shear walls*, Paper No. 978, 13th World Conference on Earthquake Engineering, Vancouver, B.C., Canada.

Wang, J., Wang, W., Xiao, Y., and Yu, B. (2019). "Cyclic test and numerical analytical assessment of cold-formed thin-walled steel shear walls using tube truss." *Thin-Walled Structures*, Vol. 134, pp. 442-459, DOI: 10.1016/j.tws.2018.09.038.

Wright, H. D. and Evans, H. R. (1995). "Profiled steel concrete sandwich elements for use in wall construction." *Proc. The 3rd International Conference on Sandwich Construction,* Southampton, UK, pp. 91-100.

Wright, H. D., Evans, H. R., and Harding, P. W. (1987). "The use of profiled steel sheeting in floor construction." *Journal of Constructional Steel Research*, Vol. 7, No. 4, pp. 279-295, DOI: 10.1016/0143-974X(87)90003-4.

Yadollahi, Y., Pakar, I., and Bayat, M. (2015). "Evaluation and comparison of behavior of corrugated steel plate shear walls." *Latin American Journal of Solids and Structures*, Vol. 12, No. 4, pp. 763-786, DOI: 10.1590/1679-78251469.

Yan, J. B., Li, Z. X., and Wang, T. (2018). "Seismic behaviour of double skin composite shear walls with overlapped headed studs." *Construction and Building Materials*, Vol. 191, pp. 590-607, DOI: 10.1016/j.conbuildmat.2018.10.042.

Yang, Y., Liu, J., and Fan, J. (2016). "Buckling behavior of double-skin composite walls: An experimental and modeling study." *Journal of Constructional Steel Research*, Vol. 121, pp. 126-135, DOI: 10.1016/j.jcsr.2016.01.019.

Zhang, W., Mahdavian, M., and Yu, C. (2018). "Lateral strength and deflection of cold-formed steel shear walls using corrugated sheathing." *Journal of Constructional Steel Research*, Vol. 148, pp. 399-408, DOI: 10.1016/j.jcsr.2018.06.009.

Zimmermann, R., Klein, H., and Kling, A. (2006). "Buckling and postbuckling of stringer stiffened fiber composite curved panels-tests and computations." *Composite Structures*, Vol. 73, No. 2, pp. 150-161, DOI: 10.1016/j.compstruct.2005.11.050.